

4. L. M. HOGAN, R. W. KRAFT and F. D. LEMPKEY, in "Advances in Materials Research", Vol. 5, edited by H. Herman (Wiley, New York, 1971) p. 83.

T. E. PEDERSEN*

M. NOACK

J. D. VERHOEVEN

*Ames Laboratory-USDOE,
and Department of Materials Science
and Engineering,
Iowa State University,
Ames, Iowa 50011,
USA*

*Received 11 December 1979
and accepted 11 January 1980*

*Present address: Bendix, Kansas City, Missouri, USA.

Penetration resistance of a magnesium casting alloy

The low density of magnesium alloys has encouraged investigations into their performance as armour materials [1]. Previous work has shown that fracture is a problem, and that one way of avoiding this is to alloy the magnesium to change the crystal structure. An alternative is to support the armour with ductile back-up plates to inhibit brittle failure modes. In either case the function of the armour is to absorb the kinetic energy of the projectile and this requires plastic flow at the highest possible flow stress. Lightweight armours thus require a high ratio of strength to density. The investigation described in this report seeks to assess the influence of microstructural changes on the ballistic performance of a typical magnesium casting alloy.

The alloy chosen was the general purpose casting alloy BS2970 MAG 1 [2] which has the nominal composition in weight per cent, 8% Al, 0.5% Zn, 0.3% Mn and the balance magnesium. The alloys were sand cast into moulds 200 mm by 200 mm, of thickness 18 mm, heavily chilled at one end; they were stress-relieved for 3 h at 260°C after casting. Radiographs showed the castings were very low in porosity.

Mechanical and ballistic tests were carried out on the alloys in three conditions: (a) as-cast and stress-relieved, (b) solution-treated, and (c) aged. The solution treatment involved heating for 8 h at 385°C and 16 h at 420°C followed by an air cool [3]. Ageing was for 1 h at 280°C following the solution treatment.

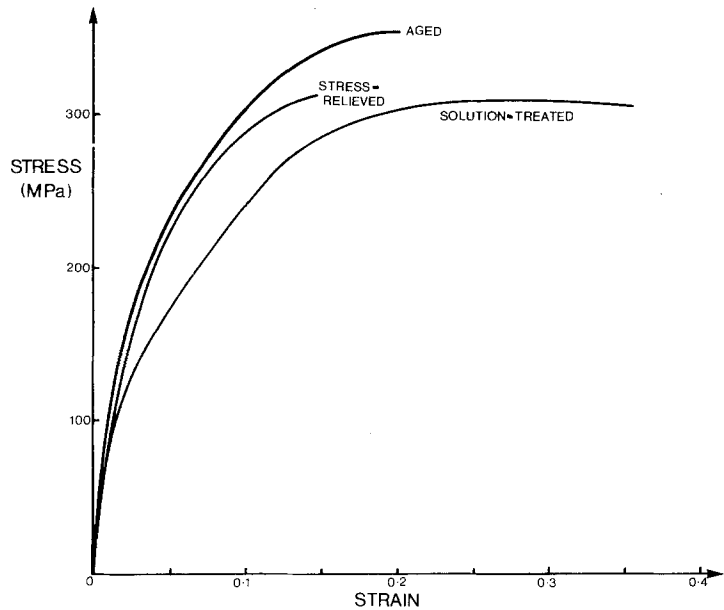
Stress/strain characteristics were determined

using uniaxial compression tests on samples in the three conditions. Ballistic tests involved the use of 4.8 mm diameter conical penetrators with an included angle of 45° at the tip, a maximum tip diameter of 0.015 mm, and a mass of 2.83 g. The details of testing have been described previously [4]. Critical velocities to penetrate targets were determined as the mean of the highest velocity at which the projectile was stopped and the lowest velocity at which penetration was achieved. In some cases a critical velocity for fragment ejection from the rear of the targets, known as discing, was also determined in the same manner.

The stress/strain curves for the alloy in the three conditions are shown in Fig. 1. The strength did not vary a great deal with heat-treatment but the ductility changed markedly. The hardness of the alloy was 66 HV in both the as-cast, stress-relieved and the aged conditions and 58 HV in the solution-treated state. There was a slight variation in properties throughout the castings and the curves of Fig. 1 and the values of hardness represent the mean values determined from a number of tests.

Critical velocities to defeat targets of thicknesses 6.4 and 12.7 mm are given in Table I for each heat-treatment condition. For the thicker targets, it was possible to separate the velocities for fragment ejection and projectile penetration; however, with the thin targets the difference between these critical velocities was less than the error in measurement of the critical velocity. In all cases fragments were ejected from the back of the target, a typical example being that of Fig. 2a. The disced area was of irregular shape although the fracture path tended to follow planes parallel to the surface of the target (Fig. 2b), characteristic of

Figure 1 Stress/strain curves for the magnesium alloy in the as-cast, stress-relieved, the solution-treated, and the aged conditions. The curves were obtained with uniaxial compression tests and the ductility, indicated by the maximum strain in each case, was limited by fracture of the samples.



discing failure. It was possible to measure a mean diameter of the disced area by taking several readings on each sample and the values for the diameter of the disced region of Table I are significant to approximately ± 1 mm.

The discing failure of the magnesium targets is associated with the inherent brittleness of the alloy. In the as-cast condition there was considerable coring with large amounts of the brittle $Mg_{17}Al_{12}$ phase distributed at grain boundaries as a divorced eutectic (Fig. 3a). Examination of failed targets showed that the $Mg_{17}Al_{12}$ phase was easily cracked and hence its removal might reduce the incidence of discing. Solution treatment resulted in a more uniform structure (Fig. 3b), and reduced the extent of discing, as shown by the measurements of the diameter of the disced area in Table I. Discing was not completely eliminated, however, and there was only a marginal increase in penetration resistance, the result of reduced discing

combined with a concurrent slight reduction in strength during solution treatment. Whilst the amount of discing can be reduced by this heat-treatment, discing cannot be removed completely because of the brittleness of the alloy associated with its hexagonal close-packed crystal structure.

Ageing of the alloy was undertaken in the hope that an increase in strength due to precipitation hardening could be achieved without an increase in the severity of discing. As shown in Fig. 1 and Table I, an increase in strength was achieved but the amount of discing increased, with the consequence that there was no further increase in penetration resistance.

As mentioned above, the only practical measure of the magnitude of the discing was the mean diameter of the disced area on the target. The depth of discing from the back face was always slightly less than the projectile diameter but, because of the very irregular nature of the fracture,

TABLE I Summary of ballistic test results

Alloy Condition	6.4 mm thick targets		12.7 mm thick targets		
	Critical velocity. Projectile penetration (m sec ⁻¹)	Mean diameter of disced area (mm)	Critical velocity (m sec ⁻¹)		Mean diameter of disced area (mm)
		Discing	Projectile penetration		
As-cast/stress-relieved	204 \pm 10	15	332 \pm 7	352 \pm 12	13
Solution-treated	265 \pm 15	9	342 \pm 6	369 \pm 5	10
Aged	—	—	337 \pm 9	368 \pm 4	12

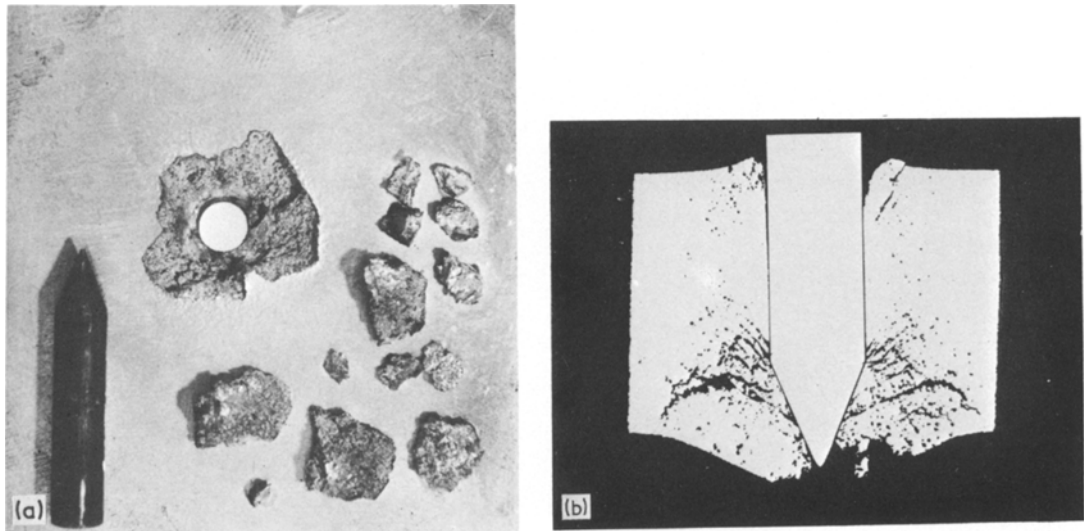


Figure 2 (a) Rear surface of a penetrated as-cast stress-relieved target, showing the discing type failure. (b) Section through a part-penetrated target, showing the propagation of the cracks parallel to the rear surface of the target to cause the discing failure. $\times 5$

it was not practical to measure the depth. The projectile cone angle and the projectile velocity were varied considerably to see if there was any correlation of these parameters with depth and diameter of discing, but any such relation was masked by the scatter of results.

The ejection of fragments from the rear of the target is a bad feature in armour applications. However, the real problem as far as penetration resistance is concerned is that the depth of the

layer involved in the discing represents a layer of target which does not have to be penetrated by the projectile. As no work is done by the projectile in plastic deformation of this rear portion of the target, the projectile effectively penetrates a target of reduced thickness, equal to the actual target thickness less the depth of discing. The potential of metals for armour applications may be assessed approximately by this density to strength ratio, ρ/σ_0 , where σ_0 is the strength coefficient in

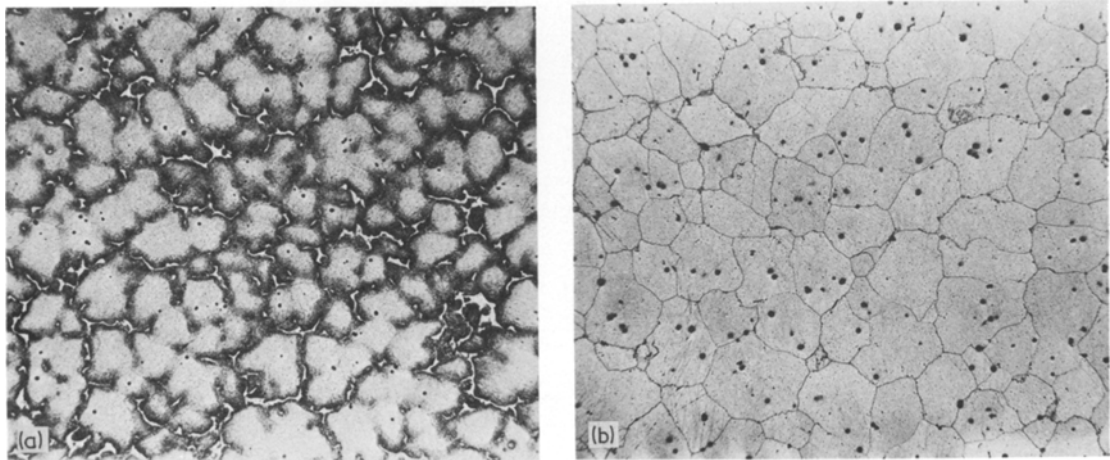


Figure 3 (a) Microstructure of the as-cast stress-relieved material, showing segregation and the brittle $Mg_{17}Al_{12}$ phase at the grain boundaries, $\times 75$. Nital etch. (b) Microstructure after solution treatment, showing the removal of the segregation, $\times 75$. Nital etch.

the curve fitting stress/strain relation $\sigma = \sigma_0 \epsilon^n$. Despite the low strength of the alloy used in the present experiments, ρ/σ_0 lies between 4 and $5 \times 10^{-6} \text{ sec}^2 \text{ m}^{-2}$ which compares well with steel and aluminium armour [5] because of the low density of magnesium. Nevertheless this assessment method assumed a ductile failure mode of the material and the present alloy does not achieve its full potential because of the discing-type failure.

There are two possible methods of overcoming the deleterious effects of discing. One approach has been to change the crystal structure by suitable alloying additions, as has been done with magnesium–lithium alloys [1]. The other technique is to hold the back of the target so that the projectile must deform the full thickness of the magnesium in order to penetrate. This can be achieved using a ductile back-up plate of sufficient stiffness that bending is limited during penetration [6]. The bending requirement means that the back-up plate must have a thickness of the order of the projectile diameter. In such a case, the penetration resistance and weight penalties must be assessed with the composite structure in mind.

Acknowledgements

The cast alloys were provided by Mr R. Dear of

the Defence Research Center, Salisbury and the heat treatment carried out by Mr I. Taylor of the Commonwealth Aircraft Corporation.

References

1. R. M. ORGORKIEWICZ, *Machine Design* 41 (27) (1969) 36.
2. British Standard 2970:1972 "Specification for Magnesium Alloy Ingots and Castings".
3. Ministry of Aviation Supply/Department of Trade and Industry, Standard DTD 690A, January 1971: "Ingots and Castings of High-Purity Magnesium–8% Aluminium–Zinc Manganese Alloy (Solution Treated)".
4. R. L. WOODWARD, *Int. J. Mech. Sci.* 20 (1978) 349.
5. *Idem*, *J. Aust. Inst. Met.* 22 (1977) 167.
6. *Idem*, *Met. Technol.* 6 (1979) 106.

Received 27 November 1979

and accepted 8 January 1980

RAYMOND L. WOODWARD

*Materials Research Laboratories,
Defence Science and Technology Organization,
P.O. Box 50, Ascot Vale,
Victoria 3032,
Australia*

Non-stoichiometry of $(\text{La}_{0.8}\text{Ca}_{0.2})\text{MnO}_{3+y}$

Several investigations of the crystal structure of the magnetic oxide $(\text{La}_{0.8}\text{Ca}_{0.2})\text{MnO}_3$ have been reported [1–6]. The present study is of the non-stoichiometry and the lattice constants of $(\text{La}_{0.8}\text{Ca}_{0.2})\text{MnO}_{3+y}$ (y : parameter of the non-stoichiometry).

The factors determining y in the preparation of the material are temperature and oxygen partial pressure and, therefore, the oxygen partial pressure was controlled with $\text{CO}_2\text{--H}_2$ or $\text{CO}_2\text{--O}_2$ mixtures [7–9]. In order to measure the relative value of y , a thermal balance of which the sensitivity is 0.1 mg was employed, and a stabilized ZrO_2 cell was used to take measurements of the oxygen partial pressures. Here, p_{O_2} (oxygen partial pressure) can be written as

(a) $\text{CO}_2\text{--H}_2$ mixture:

$$p_{\text{O}_2}(\text{MPa}) = 0.10199 \times 10^{-11}$$

$$\times \{r - 1 + [(r - 1)^2 + 4r/2.456]^{1/2}\}^2/4 \quad (1)$$

at 1473 K, where $r = p_{\text{CO}_2}(\text{i})/p_{\text{H}_2}(\text{i})$: the ratio of the initial partial pressures of CO_2 and H_2 at room temperature, and $\text{MPa} = 10^6 \text{ Nm}^{-2} = 9.869233 \text{ atm}$;

(b) $\text{CO}_2\text{--O}_2$ mixture:

$$p_{\text{O}_2}(\text{MPa}) = 0.101325(2r + f)/(2 + 2r + f), \quad (2)$$

$$f = 1.0033(1 - f)[(2 + 2r + f)/(2r + f)]^{1/2}. \quad (3)$$

Equation 3 is iterated using $f = 0$ as the initial value. The result of the iteration is substituted into Equation 2 and then p_{O_2} is obtained. When $r > 0.01$ this result is well approximated by